DTU Library

A gradient nanostructure generated in pure copper by platen friction sliding deformation

Deng, S. Q.; Godfrey, A.; Liu, W.; Hansen, Niels

Published in:
Scripta Materialia

Link to article, DOI:
10.1016/j.scriptamat.2016.02.007

Publication date:
2016

Document Version
Peer reviewed version

A gradient nanostructure generated in pure copper by platen friction sliding deformation

S. Q. Deng [1], A. Godfrey [1,*], W. Liu [1], N. Hansen [2]

1. Key Laboratory of Advanced Materials (MOE), School of Material Science and Engineering, Tsinghua University, Beijing 100084, P.R. China

2. Danish-Chinese Center for Nanometals, Section for Material Science and Advanced Characterization, Department of Wind Energy, Technical University of Denmark, 4000 Roskilde, Denmark

* Corresponding author. Tel.: +86 10 62788317; Fax: +86 10 62771160

E-mail address: awgodfrey@mail.tsinghua.edu.cn (A. Godfrey).

Abstract: A modified friction sliding process with a large applied normal load has been used to develop a gradient nanostructure in Cu using only a short processing time. A quantitative characterization of the variation in microstructure and strength has been carried out by combined use of electron backscatter diffraction and hardness measurements, and the data used to estimate the effective strain profile resulting from the processing treatment. The affected deformation volume extends to a large depth of more than 1 mm, with a top surface hardness of 2.28 GPa, corresponding to a four-fold increase compared to the initial undeformed material.

Keywords: Friction deformation; EBSD; Copper; Gradient nanostructure.

A variety of techniques for generating gradient nanostructures in metals have been investigated, including surface mechanical attrition treatment [1,2], shot-peening [3,4], surface mechanical grinding treatment (SMGT) [5], burnishing [6-8] and sliding deformation [9-13]. In this study we investigate a variant of sliding where one planar surface is moved over another while under a compressive load. In contrast to similar previously reported techniques [9,10,13] our modified platen friction sliding deformation (PFSD) process [14] involves the use of a significantly larger compressive load during sliding and an enhanced surface roughness, with the dual objectives of increasing the strain gradient introduced during deformation (as well as the near-surface hardness), and increasing the depth to which hardening takes place below the surface.

A detailed knowledge of the resulting strain gradient is important as this provides the basis for both evaluation and further development of computer models of surface deformation processes [15]. The shear strain profile (representing the material flow) can in certain cases be estimated by the use of microstructural markers, as demonstrated recently by Moering et al. [16]. Here we use quantitative microstructural data to explore an alternative approach for estimation of the effective strain profile, representing the equivalent strain in bulk deformation resulting in the same microstructural scale and hardness. This is a more general approach and provides information on the combination of the shear strain gradient, together with the local strain rate gradient (and hence any heating) and the material chemistry.

For this purpose we use the electron backscatter diffraction (EBSD) technique for microstructural characterization. This has the advantage of allowing examination of large areas of material, and is therefore less sensitive to variations in the microstructure along the sliding direction at any given depth than transmission electron microscope-based observations. Additionally this technique allows a direct correlation of hardness measurements with the local microstructural characteristics.

As a model material, and to allow comparison with previous studies of friction sliding under different conditions [9,10,13,17-20] oxygen-free high conductivity Cu (99.9% purity) was used in this study. The initial material was in a fully recrystallized condition with an average grain size of 73 μm (determined ignoring annealing twins) and a nearly random texture. As illustrated schematically in Fig. 1a the PFSD system consists of two perpendicularly arranged loading frames. The sample is held with the outer surface in full contact with the friction platen (in this experiment a hardened steel bar) under a compressive load, applied using the horizontal loading frame. The compressive force is controlled using a load cell placed in line with the sample, on the opposite side of the friction platen. The sample is fully supported on its underside to prevent slippage during the friction sliding process. The friction platen is held by a separate vertical loading frame, which is used to push the platen down, resulting in deformation to the surface of the sample. The maximum sliding distance that can be achieved in one pass is determined by the space available for travel of the platen, which in our case was 60 mm.

In this study, Cu samples of size 11.5 x 11.5 x 9 mm^3 were used, with the square face of the sample placed against the friction platen (of size 32 x 32 x 100 mm^3). The PFSD process was carried out at room temperature using a normal (compressive) stress of 44 MPa, a platen-sliding speed of 6.7 mm s^{-1}, and a sliding distance of 60 mm. In order to highly refine the microstructure the PFSD process was repeated using four passes over the same area (resulting in a total sliding distance of ≈ 240 mm and a total deformation time of less than one minute). Moderately high values of initial surface roughness for both the Cu sample and the friction platen were chosen (measured as Ra=5.1 μm and Ra=3.2 μm, respectively). The effect of surface roughness on the PFSD process is described elsewhere [21]. After deformation all samples were held at -18 °C in a freezer to prevent recovery and recrystallization during storage.

The microstructure resulting from PFSD was examined on polished cross-sections (perpendicular to the sliding surface, and containing the sliding direction), and was characterized using a Tescan Mira 3 LMH thermal field emission scanning electron microscope (FE-SEM) equipped with an Oxford Instruments HKL Nordlys Max EBSD system. The strength was estimated from Vickers micro-hardness indentations, using a load of 10 g and a load duration of 10 s on the same cross-sections. These values resulted in indent sizes in the uppermost volumes in the range of 9 – 12 μm. Accordingly in the top 100 μm of the sample hardness indents were taken at 10 μm intervals, but offset from each other along the sliding direction to achieve a minimum spacing between indents of ≈ 30 μm. The indent in the cross section nearest the top surface was taken at a depth of 12 μm. To allow an estimation of the strain gradient introduced during PFSD, samples of the same initial material were also deformed by cold-rolling to a large von Mises strain of $\varepsilon_{vM} = 5.2$, and then examined using similar techniques.

Figures 1(b-e) and 2 give an overview of the microstructural observations of the sample after PFSD, based on SEM and EBSD examination, respectively. As seen in Fig. 1b, a clear microstructural gradient is developed after PFSD. A large amount of plastic deformation is introduced in the top ≈ 100 μm, where the original grain boundaries can no longer be recognized. The microstructural morphology varies considerably, however, in a non-continuous manner, with depth from the friction surface. Near the top surface (Fig. 1c) the microstructure is composed of fine nanoscale lamellae lying nearly parallel to the sliding direction, with an average spacing of about 50-100 nm,. Below this, the microstructure is composed of fine grains extended along the sliding direction (Fig. 1d). At greater depths the microstructure resembles a regular lamellar deformation microstructure, with elongated bands either parallel, or at a shallow angle, to the sliding direction (Fig. 1e). At still greater depths the initial grains can still be clearly identified, with some evidence of some plastic deformation inside the grains.

Based on both the FE-SEM and EBSD observations four depth regions, each with a typical microstructure, can be identified, as shown in Fig. 2. Region I (0 - 15 μm depth) is composed of a nanoscale lamellae microstructure. These nanoscale lamellae are mostly non-indexed in the EBSD maps, due to the high deformation level and their fine spacing. Region II (15 - 50 μm depth) consists of fine grains, extended along the sliding direction (Fig. 2a). The EBSD data confirm that these grains are mostly separated by high angle boundaries. Region III (50

- 120 μm depth) consists of a regular lamellar deformation microstructure. It is seen that this structure becomes coarser with increasing depth from the friction surface. Region IV (> 120 μm depth) is composed of the mildly deformed initial grains. Similar to near-surface structures seen during wear [18-20], the transition from region I to region II is markedly discontinuous, though in the present case region I extends to a much greater depth of 15 μm.

The hardness (Hv) profile, measured in the sample cross-section at different depths from the friction surface, is plotted in Fig. 3a. Also shown is the hardness value at 0 μm depth and the hardness of the initial Cu before PFSD. The hardness profile shows a good correspondence to the microstructure, with hardness decreasing with increasing depth, from about Hv = 2.28 GPa at the friction surface (0 μm depth) to about Hv = 1.04 GPa at a depth of 100 μm, then decreasing slowly after this with further depth. The hardness values at the friction surface and near the base of region I (12 μm depth; Hv = 1.87 GPa) are very high – 4 times and 3.3 times that of the Cu before PFSD (Hv = 0.56 GPa), respectively. The dashed curve in Fig. 3a shows the result of fitting the hardness values to a power-law of the form Hv = $2.9d^{-0.21}$, where d is the distance from the top surface. Although the overall fit is good (R^2 = 0.97), closer inspection shows systematic deviations that reflect the transitions in microstructure from regions I to IV.

The variation in boundary spacing (D_{av}) as a function of depth from friction surface has also been determined from the EBSD data. Values of D_{av} were taken from line scans along the direction perpendicular to the sliding direction, considering misorientation angle (θ) definitions both of ≥ 1.5° and ≥ 15°. The results are shown in Fig. 3b, where the error bar represents the thickness of the layer used to determine the D_{av} at each depth. The values of D_{av} increase with increasing depth from friction surface, as expected for a gradient structure. Region II exhibits a noticeably smaller variation in D_{av}, which combined with the large fraction of high angle boundaries and the more equiaxed grain shape compared to that in deeper layers, strongly suggests that the microstructure in this region results from a process of dynamic recovery and/or recrystallization, as has been seen previously in wear layers and friction deformation [17,22,23]. The formation of relatively large volume of such material in the present case, extending over 30 – 40 μm can be understood based on the balance of heat generation due to the high local shear strain rate during PFSD, combined with the large thermal mass provided by the base material.

The hardness and boundary spacing data have also been combined to probe the strength-structure relationship in the deformed material. This is done here for the depth of up to 100 μm, where the EBSD data for boundary spacing are considered most reliable. As seen in Fig. 3c the data can be described by a Hall-Petch plot with a slope (k_{HP}) of ≈ 180 MPa $\mu m^{0.5}$, calculated assuming σ = HV/3.3 and a value of σ_0 = 20 MPa. The slope is slightly higher than that found for bulk Cu (k_{HP} = 140 MPa $\mu m^{0.5}$), as expected given that it is not possible using EBSD data to separate the contribution of grain boundary strengthening from Taylor strengthening due to loose dislocations and low angle boundaries in the deformed structure [24]. Similarly, although the spacing of the nanoscale lamellae near the top surface cannot be determined from the EBSD maps, based on a value of the Hall-Petch coefficient for Cu of between 140 and 180 MPa $\mu m^{0.5}$, the measured hardness (1.87 GPa) corresponds to a boundary spacing of between 65 nm and 110 nm, which agrees with the FE-SEM observations.

To estimate the effective strain profile as a function of depth in the samples treated by PFSD two approaches have been used. Firstly, following Zhang et al. [24], by use of a master curve for boundary spacing as a function of strain for samples of the same initial Cu material deformed by cold rolling to a high strain of ε_{vM}= 5.2 (Fig. 4a). In each case the spacing was determined from EBSD measurements using a boundary misorientation definition of 1.5°. Secondly, by use of hardness measurements, again using cold-rolled (CR) samples to provide a calibration curve (Fig. 4a).

The resulting strain-depth profiles for the PFSD-treated samples are shown in Fig. 4b. The two curves show some differences, but nevertheless have a very similar shape for depths greater than 50 μm, and highlight that some deformation takes place to depths of up to 3 mm during the PFSD process. It can be noted in particular that the comparison based on hardness data assumes that work hardening of a gradient structure can be equated directly to that in the cold-rolled sample, and in both cases the influence of any change in metal chemistry by mixing of impurities is neglected, though this is likely only to be important at the near-surface layer. Accordingly the measured hardness at the friction surface is not used in Fig. 4. For similar reasons, the boundary spacing in region I, where nanoscale lamellae are found to form, has not been used for estimation of strain in the plot. It should be noted also that the strain-depth profile based on spacing is only determined to a depth of approx. 100 μm, as at greater depths the boundary spacing cannot be determined reliably from the EBSD data. The shear strain has also been estimated at locations where the shearing of the microstructural features within each grain can be clearly identified. These estimates, based on the shearing of either twin boundaries or deformation microbands, are marked in Fig. 4b. It is seen that at depths of at least 90 μm the effective strain follows closely the physical shear strain, which gives confidence to the use of the master curve based on the EBSD data. The divergence of the curves based on hardness and microstructure reflects the complex nature of the deformation in the near-surface region, where the physical shear strain may exceed 100 [13].

Figure 4c compares the strain-depth profile in the top 200 μm layer for PFSD with those reported previously for friction-sliding deformation of copper using lower normal loads [10] (obtained from measurements of the shearing of microstructural markers) and for shot-peening of iron [24] (obtained using hardness data). It is seen that the strain-depth profile obtained from Hv data follows a similar shape to the previously reported curves, but that the larger applied load results in larger strain at any depth, and a deeper deformation-affected zone. Interestingly, the PFSD strain-depth profile obtained from boundary spacing is similar to that found for shot peening [24], though the total processing time for PFSD is only a fraction of that for shot peening.

In summary, it is found that modified friction sliding process, using a relatively large applied load, can be used to generate rapidly a gradient nanostructure in Cu at room temperature, with a deformation time of less than one minute. With increasing depth from friction surface, a non-uniform increase in the microstructural scale is found, in particular a sharp transition from a 15 μm nanostructured top layer to an extended region of fine grains where the grain size increases only slowly with depth. The change in hardness reflects the microstructural varation, falling rapidly from Hv = 2.28 GPa at the friction surface to Hv = 1.04 GPa at a depth of 100 μm, with the deformation-affected volume extending to a depth of up to 3 mm below the sample surface. It is shown additionally how the microstructure and hardness measurements also allow an estimation of the effective strain-depth profile resulting from surface deformation process, providing complimentary data to measurements of shear strain based on material flow. In the present work Cu has been used as a model material. The process can nevertheless be applied to engineering materials for use under conditions of wear and friction, with the only requirement being that the friction-platen should be of sufficient strength. It can be concluded that PFSD provides a rapid and highly efficient method for introduction of a gradient nanostructure at the surface of metal samples of both fundamental and applied interest.

The authors gratefully acknowledge the support from the Danish National Research Foundation (Grant No. DNRF86-5) and the National Natural Science Foundation of China (Grant No. 51261130091) to the Danish–Chinese Center for Nanometals, and to the National Natural Science Foundation of China (Grant No. 51171085).

[1] K. Lu, J. Lu. Mater Sci. Eng. A 375 (2004) 38.
[2] X.L. Wu, N.R. Tao, Q.M. Wei, P. Jiang, J. Lu, K. Lu. Acta Mater. 55 (2007) 5768.
[3] A.L. Ortiz, J.W. Tian, L.L. Shaw, P. K. Liaw. Scripta Mater. 62 (2010) 129.

[4] M. Thomas, M. Jackson. Scr. Mater. 66 (2012) 1065.
[5] W.L. Li, N.R. Tao, K. Lu. Scr. Mater. 59 (2008) 546.
[6] X. Zhang, H. Luo, Z. Han, J. Lv. Mater. Sci. Technol. 30 (2014) 1742.
[7] V.P. Kuznetsov, I.Y. Smolin, A.I. Dmitriev, S.Y. Tarasov,V.G. Gorgots. Surf. Coat. Technol. 285 (2016) 171.
[8] P. Balland, L. Tabourot, F. Degre, V. Moreau. Precis. Eng. 37 (2013) 129.
[9] D.A. Hughes, D.B. Dawson, J.S. Korellis, L.I. Weingarten. J. Mater. Eng. Perform. 3 (1994) 459.
[10] D.A. Hughes, D.B. Dawson, J.S. Korellis, L.I. Weingarten. Wear 181 (1995) 458.
[11] Y.S. Zhang, P.X. Zhang, H.Z. Niu, C. Chen, G. Wang, D.H. Xiao, X.H. Chen, Z.T. Yu, S.B. Yuan, X.F. Bai. Mater. Sci. Eng. A 607 (2014) 351.
[12] H.J. Kim, A. Emge, R.E. Winter, P.T. Keightley, W.K. Kim, M.L. Falk, D.A. Rigney, Acta Mater. 57 (2013) 5270.
[13] D.A. Hughes, N. Hansen. Phys. Rev. Lett. 112 (2014).
[14] S.Q. Deng, A. Godfrey, W. Liu, C.L. Zhang. Mater Sci. Eng. A 639 (2015) 448.
[15] H.S Liu, X.D. Zhang, Hansen N., Y.K. Gao, in Proc. 35th Risø International Symposium on Materials Science, Ed. S. Faester et al., Technical University of Denmark, Roskilde (2014) 381.
[16] J. Moering, X.L. Ma, G.Z. Chen, P.F. Miao, G.Z. Li, G. Qian, S. Mathaudhu, Y.T. Zhu, Scripta Mater 108 (2015) 100.
[17] J.H. Dautzenberg. Wear 60 (1980) 401.
[18] P. Heilmann, W.A. Clark, D.A. Rigney. Acta Metall. 31 (1983)1293.
[19] D.A. Rigney, R. Divakar, S.M. Kuo. Scr. Metall. Mater. 27 (1992) 975.
[20] A. Emge, S. Karthikeyan, D.A. Rigney. Wear 267 (2009) 562.
[21] S.Q. Deng, A. Godfrey, W. Liu, C.L. Zhang, B. Xu. Accepted for publication in Int. J. Min. Met. Mater. (2015).
[22] S.M. Kuo, D.A. Rigney. Mater. Sci. Eng. A 157 (1992) 131.
[23] B. Yao, Z. Han, K. Lu. Wear 294-295 (2012) 438.
[24] X. Zhang, N. Hansen, Y. Gao, X. Huang. Acta Mater. 60 (2012) 5933.

Figure captions:

Fig. 1. (a) Schematic illustration of the PFSD set-up; (b-e) SEM micrographs of the Cu sample after PFSD, showing (b) the transition from highly refined surface to deformed grains in the top 400 μm of the sample; (c) nanoscale lamellae at 10 μm depth; (d) fine-grain structure at 30 μm depth; and (e) regular deformation lamellae at 90 μm depth. The arrow indicates the sliding direction of the friction platen. Direct evidence of shearing can be observed to at least a depth of about 160 μm, based on the curving of microstructural features such as twin boundaries and deformation bands towards the sliding direction.

Fig. 2. Typical microstructural morphologies of Cu after PFSD as observed in cross-section by EBSD: (a) top 70 μm, showing the transition from nanoscale lamellae (region I, seen as the mostly non-indexed region), to fine grains (region II), to a regular lamellar deformation structure (region III); (b) the regular lamellar deformation structure (region III) at depth of 70-120 μm; (c) deformed grains (region IV) at a depth of 400-900 μm. The arrow indicates the sliding direction of the friction platen. Adjacent pixel misorientations of ≥1.5° and ≥15° are indicated by light grey and black lines, respectively.

Fig. 3. Profiles as a function of depth from the friction surface of (a) hardness, and (b) average boundary spacing (D_{av}) along a direction normal to the sliding surface for misorientation angle definitions of θ = 1.5 and 15 °. In (a) the horizontal dashed line shows the hardness of the initial material; the dashed curve is a fit of the data to a simple power law

expression. The inset shows the change in hardness in the top 200 μm layer; (c) Hall-Petch plot relating spacing and yield stress for depths between 20 and 100 μm.

Fig. 4. (a) Variation of Hv and D_{av} with von Mises strain for cold-rolled Cu; (b) estimated effective strain-depth profile for the PFSD processed Cu sample based on either spacing (D_{av}) or hardness (Hv). The hollow blue symbols show estimates of physical shear strain based on shearing of microstructural markers (microbands, twin, and microbands at depths of 90, 110, and 130 μm respectively). The inset shows a magnified region of the Hv-based estimate using a log scale to show that strain is imparted to a depth of more than 1 mm; (c) comparison of the strain-depth profiles for PFSD with those reported for friction sliding of Cu under lower applied loads [10] and with the profile obtained for shot-peening of Fe [24].

***Graphical Abstract**

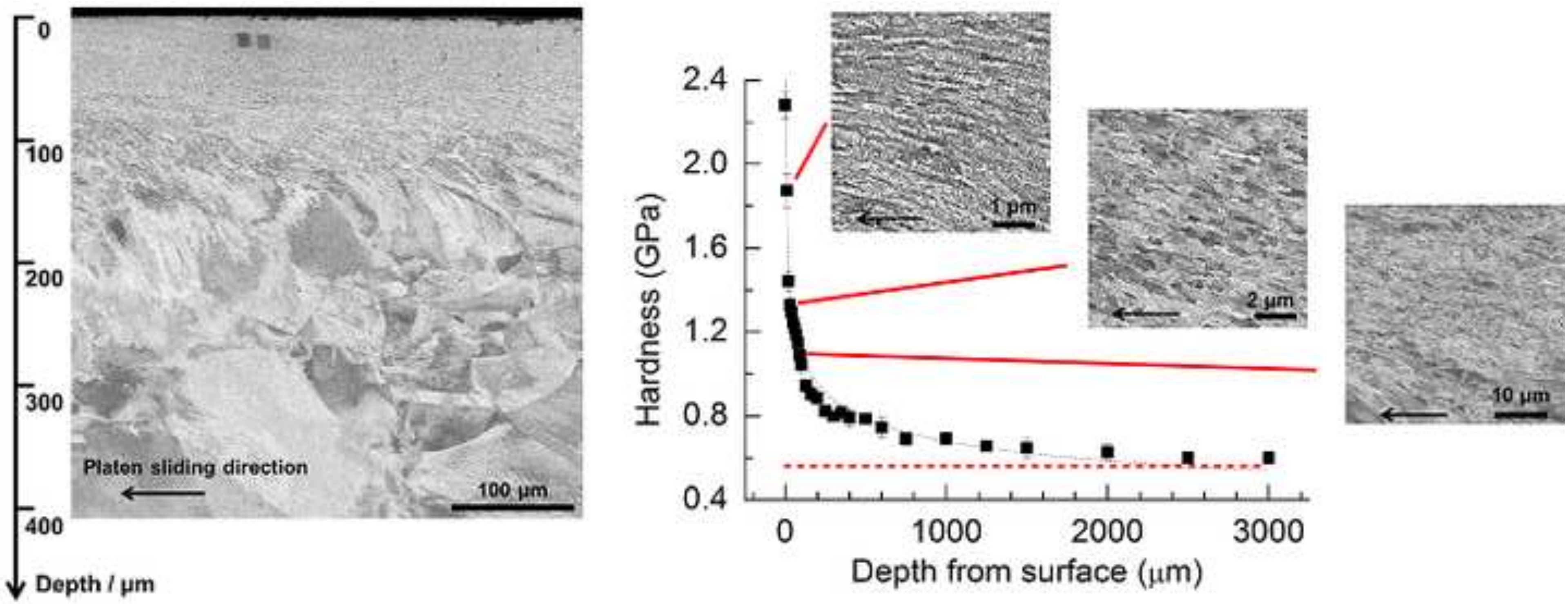

Fig 1
Click here to download high resolution image

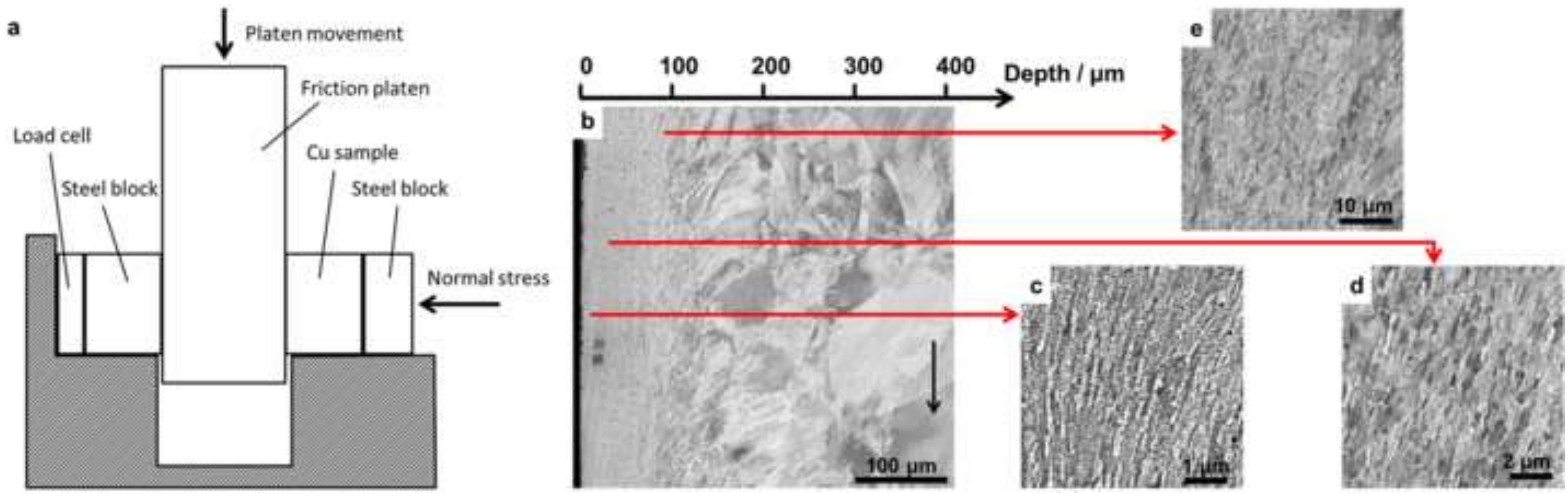

Fig 2
Click here to download high resolution image

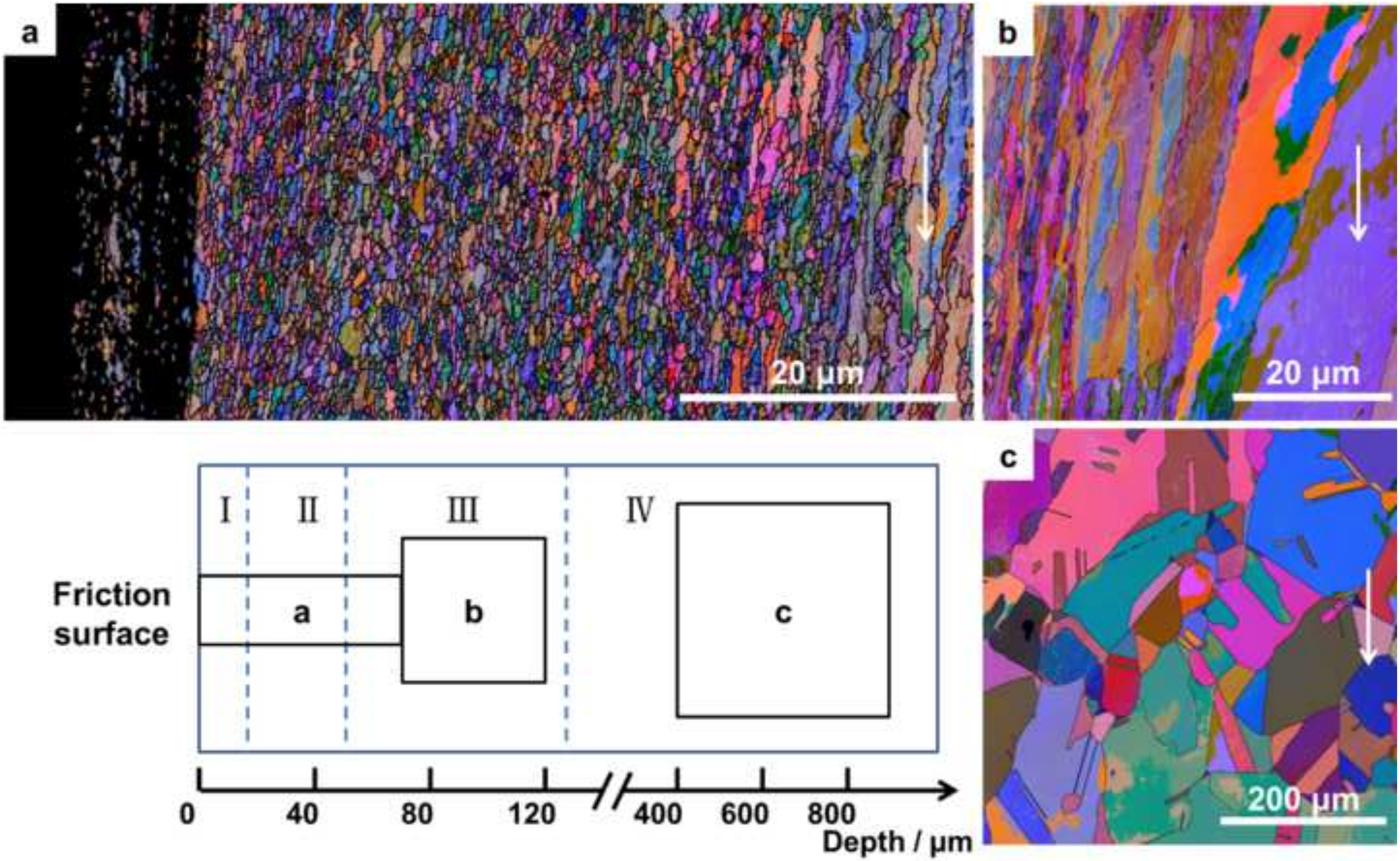

Fig 3a
Click here to download high resolution image

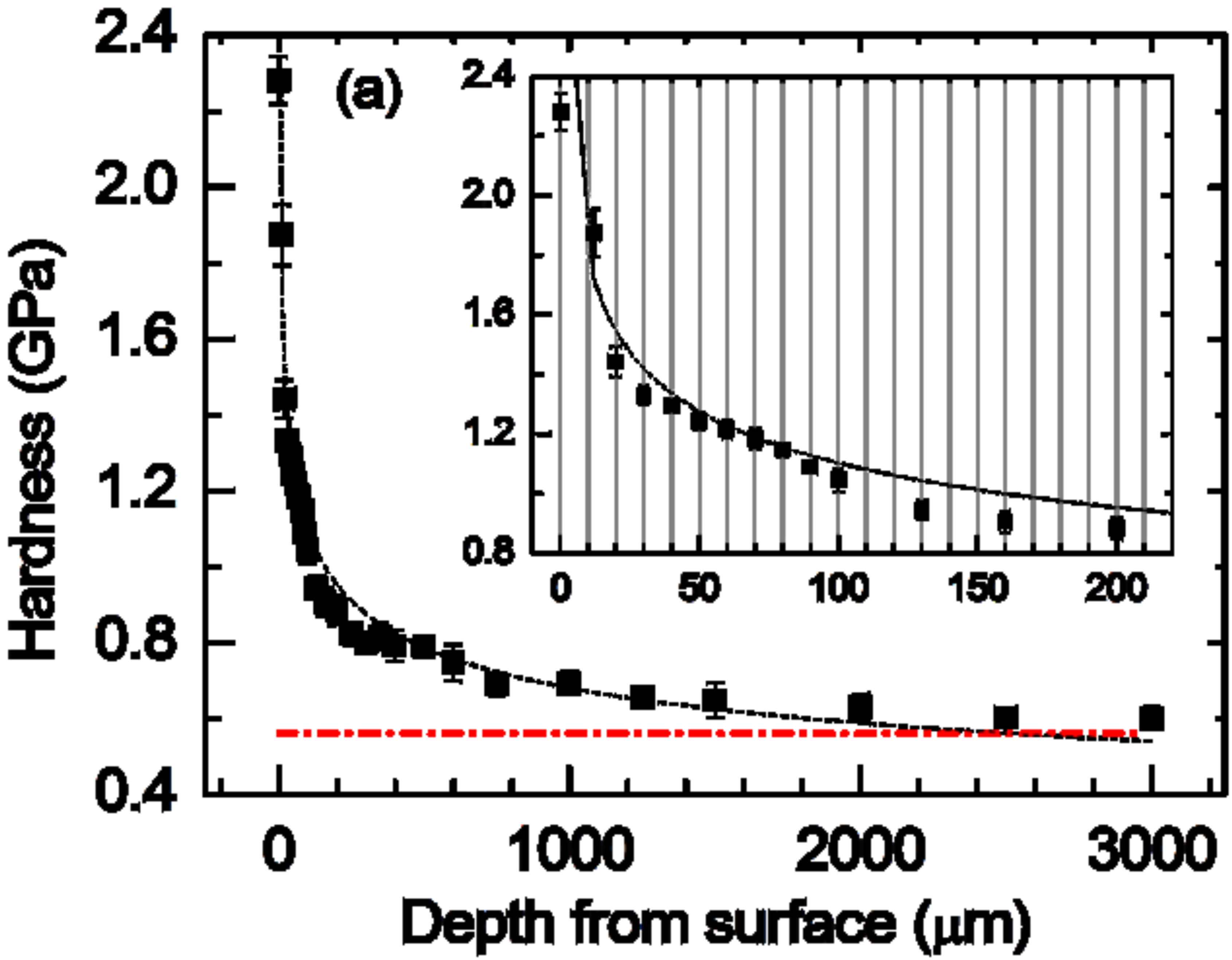

Fig 3b
Click here to download high resolution image

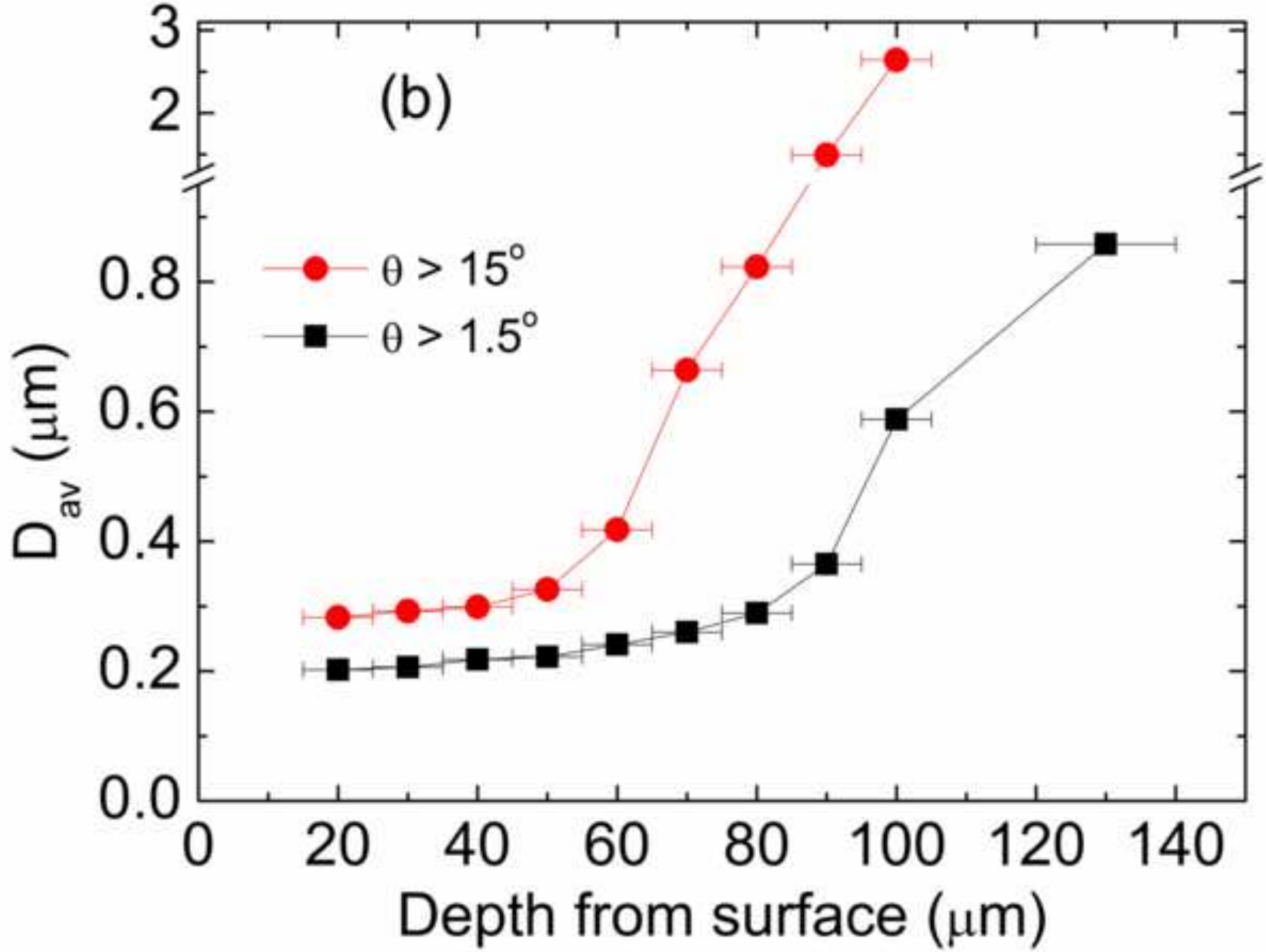

Fig 3c
Click here to download high resolution image

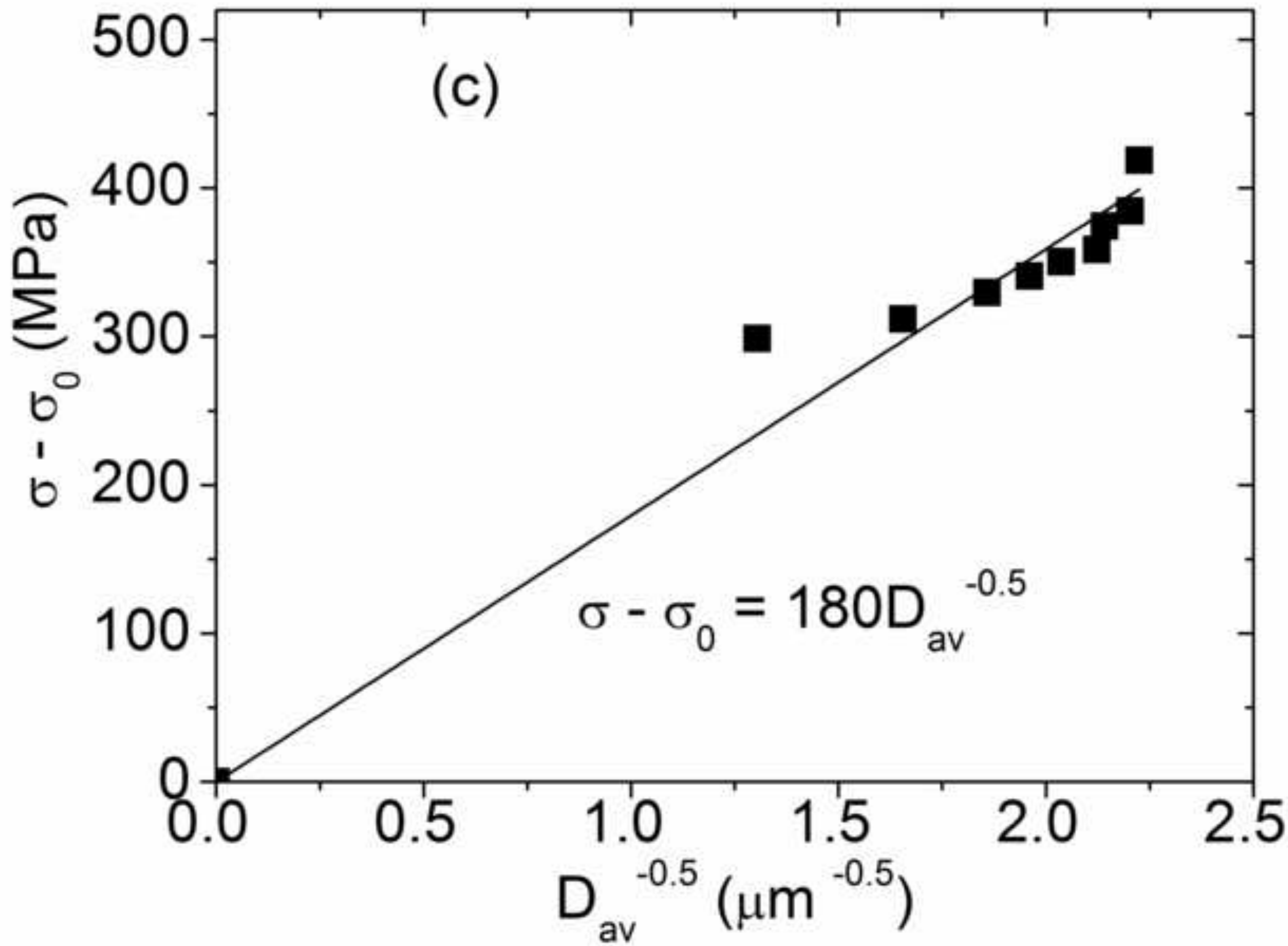

Fig 4a
Click here to download high resolution image

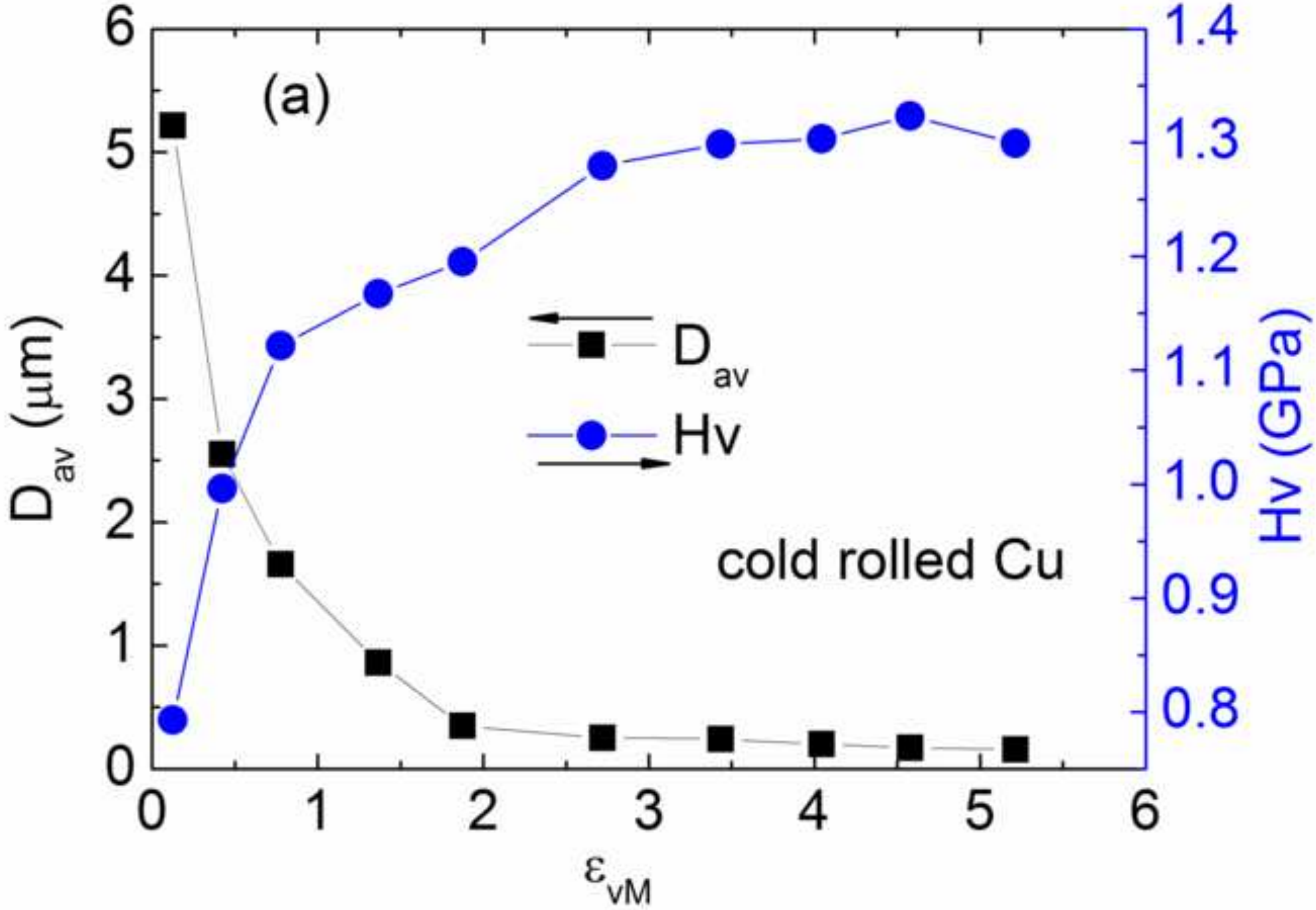

Fig4b
Click here to download high resolution image

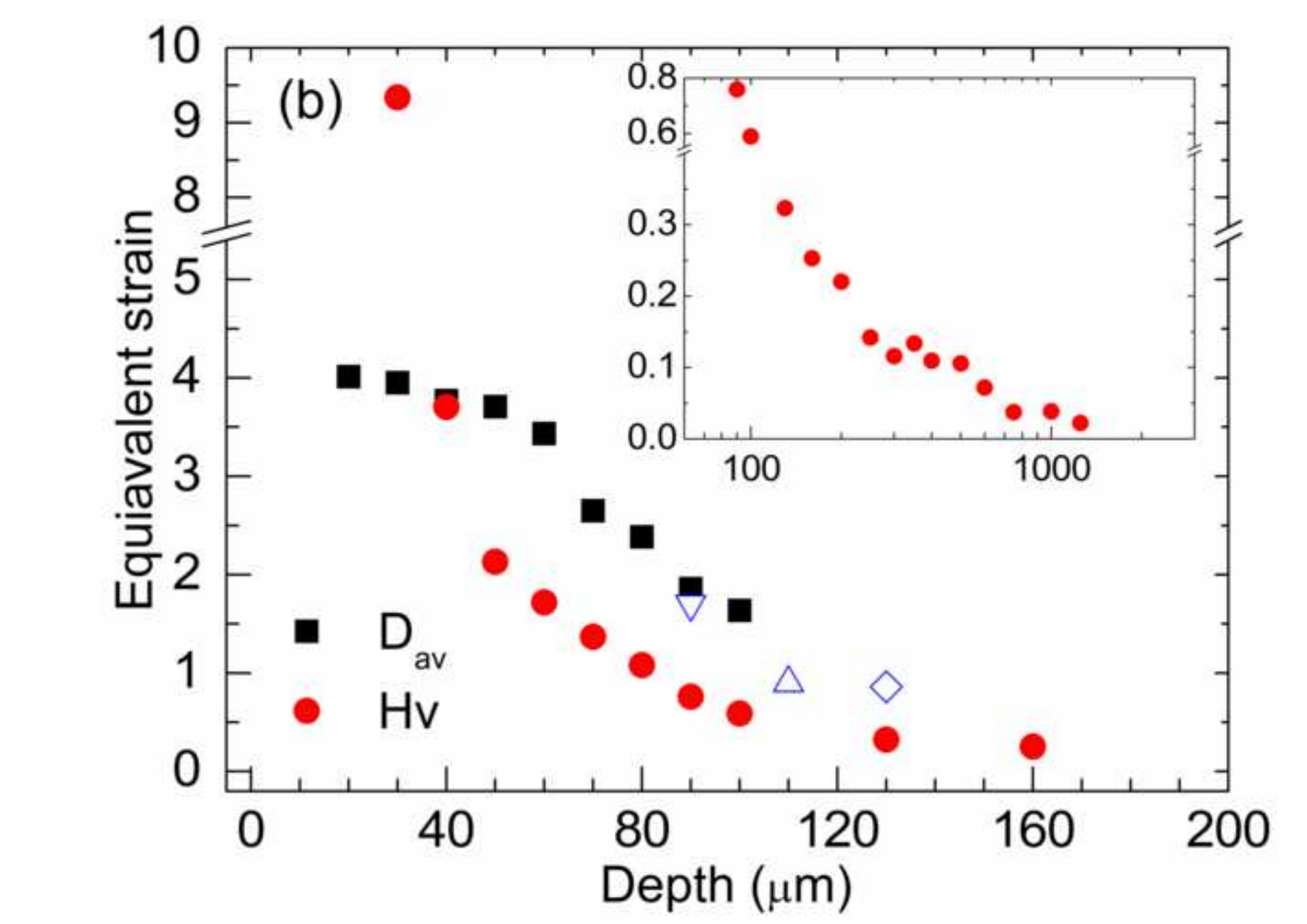

Fig 4c
Click here to download high resolution image